Raman Study of Uncoated and p-BN/SiC-Coated Hi-Nicalon Fiber Reinforced Celsian Matrix Composities

Part 2: Residual Stress in the Fibers

Gwénaël Gouadec
CNRS and ONERA, France

Philippe Colomban
CNRS, France

Narottam P. Bansal
Glenn Research Center, Cleveland, Ohio

September 2000

Since its founding, NASA has been dedicated to the advancement of aeronautics and space science. The NASA Scientific and Technical Information (STI) Program Office plays a key part in helping NASA maintain this important role.

The NASA STI Program Office is operated by Langley Research Center, the Lead Center for NASA's scientific and technical information. The NASA STI Program Office provides access to the NASA STI Database, the largest collection of aeronautical and space science STI in the world. The Program Office is also NASA's institutional mechanism for disseminating the results of its research and development activities. These results are published by NASA in the NASA STI Report Series, which includes the following report types:

- TECHNICAL PUBLICATION. Reports of completed research or a major significant phase of research that present the results of NASA programs and include extensive data or theoretical analysis. Includes compilations of significant scientific and technical data and information deemed to be of continuing reference value. NASA's counterpart of peer-reviewed formal professional papers but has less stringent limitations on manuscript length and extent of graphic presentations.

- TECHNICAL MEMORANDUM. Scientific and technical findings that are preliminary or of specialized interest, e.g., quick release reports, working papers, and bibliographies that contain minimal annotation. Does not contain extensive analysis.

- CONTRACTOR REPORT. Scientific and technical findings by NASA-sponsored contractors and grantees.

- CONFERENCE PUBLICATION. Collected papers from scientific and technical conferences, symposia, seminars, or other meetings sponsored or cosponsored by NASA.

- SPECIAL PUBLICATION. Scientific, technical, or historical information from NASA programs, projects, and missions, often concerned with subjects having substantial public interest.

- TECHNICAL TRANSLATION. English-language translations of foreign scientific and technical material pertinent to NASA's mission.

Specialized services that complement the STI Program Office's diverse offerings include creating custom thesauri, building customized data bases, organizing and publishing research results . . . even providing videos.

For more information about the NASA STI Program Office, see the following:

- Access the NASA STI Program Home Page at *http://www.sti.nasa.gov*

- E-mail your question via the Internet to help@sti.nasa.gov

- Fax your question to the NASA Access Help Desk at (301) 621-0134

- Telephone the NASA Access Help Desk at (301) 621-0390

- Write to:
  NASA Access Help Desk
  NASA Center for AeroSpace Information
  7121 Standard Drive
  Hanover, MD 21076

NASA/TM—2000-210456

Raman Study of Uncoated and p-BN/SiC-Coated Hi-Nicalon Fiber Reinforced Celsian Matrix Composities

Part 2: Residual Stress in the Fibers

Gwénaël Gouadec
CNRS and ONERA, France

Philippe Colomban
CNRS, France

Narottam P. Bansal
Glenn Research Center, Cleveland, Ohio

National Aeronautics and
Space Administration

Glenn Research Center

September 2000

Available from

NASA Center for Aerospace Information
7121 Standard Drive
Hanover, MD 21076
Price Code: A03

National Technical Information Service
5285 Port Royal Road
Springfield, VA 22100
Price Code: A03

Available electronically at http://gltrs.grc.nasa.gov/GLTRS

RAMAN STUDY OF UNCOATED AND p-BN/SiC-COATED Hi-NiCALON FIBER REINFORCED CELSIAN MATRIX COMPOSITES
PART 2: RESIDUAL STRESS IN THE FIBERS

Gwénaël Gouadec[1,2]
CNRS and ONERA
France

Philippe Colomban[1]
CNRS
France

Narottam P. Bansal
National Aeronautics and Space Administration
Glenn Research Center
Cleveland, Ohio 44135

SUMMARY

Band shifts on Raman spectra were used to assess, at a microscopic scale, the residual strain existing in Hi-Nicalon fibers reinforcing celsian matrix composites. Uncoated as well as p-BN/SiC- and p-B(Si)N/SiC-coated Hi-Nicalon fibers were used as the reinforcements. We unambiguously conclude that the fibers are in a state of compressive residual stress. Quantitative determination of the residual stress was made possible by taking into account the heating induced by laser probing and by using a reference line, of fixed wavenumber. We found fiber compressive residual stress values between 110 and 960 MPa, depending on the fiber/matrix coating in the composite. A stress relaxation-like phenomenon was observed at the surface of p-BN/SiC-coated Hi-Nicalon fibers whereas the uncoated or p-B(Si)N/SiC-coated Hi-Nicalon fibers did not show any stress relaxation in the Celsian matrix composites.

INTRODUCTION

Ceramic matrix composites (CMCs) are light-weight refractory materials which are of potential interest for high-temperature structural components in various aerospace and industrial applications. In part I, (ref. 1) the phases present in celsian matrix composites reinforced with (desized) uncoated or p-BN/SiC-coated Hi-Nicalon fibers were identified and characterized by Raman microspectroscopy, from a chemical and structural point of view. In this second part, we further interpret the fibers' spectra in an attempt to assess the residual strain resulting from the difference in coefficient of thermal expansion, α, between the fiber and the matrix. Modeling this stress mathematically would be difficult, especially in the case of coated fibers. Indeed, interphase materials promote stress relaxation (due to higher compliance, cracking or α mismatch). Besides, they are usually partly crystalline, often metastable, materials and their expansion is difficult to measure. The objective of this paper is to assess stresses in Hi-Nicalon fibers embedded in celsian matrix composites using Raman microspectroscopy.

BACKGROUND

Raman-based stress measurements rely on the anharmonic nature of the chemical bonds, which make normal vibrations sensitive to any external disturbance of the potential well, say for instance a pressure or a temperature change

---

(ref. 2). The shift induced on mode i wavenumber v_i (cm^{-1}) when a stress σ (GPa) is applied to the material is calibrated by linear regression:

$$v_i = v_i^0 + S_i^\sigma \times \sigma \tag{1}$$

where v_i^0 is the "stress-free wavenumber" and S_i^σ, expressed in cm^{-1}/GPa unit, is a direct measure of bond anharmonicity (refs. 3 and 4). Adopting the convention that σ is positive for a compressive stress, S_i^σ is positive in almost all cases and depends on the mode according to the structure anisotropy.

Many of the available values were obtained through diamond anvil cell experiments on crystals, σ being the hydrostatic pressure. Examples of investigated materials are diamond (ref. 5), fullerites (refs. 6 and 7), 6H-SiC (refs. 8 and 9), ilmenite (ref. 10) and TiO$_2$ (ref. 11). Some data also exist for materials stressed uniaxially, either in compression (diamond (ref. 12), silicon (ref. 13), Ti$_2$O$_3$ (ref. 14), sapphire (ref. 14), CaF$_2$ (ref. 15), BaF$_2$ (ref. 15), Bi$_{12}$GeO$_{20}$ (ref. 15)) or in tension (silica (ref. 16)). These reported values cannot be applied to multiphase materials like SiC fibers, because the phases are amorphous/nano-crystalline (ref. 17). Wavenumber shift calibrations are then mandatory, and usually obtained under axial tension. The control parameter is the strain $\varepsilon^\%$ (the superscript % is a reminder that we do not use the "absolute" strain), which leads to a sensitivity expressed in cm^{-1}/% unit (refs. 18 to 21):

$$v_i = v_i^0 + S_i^\varepsilon \times \varepsilon^\% \tag{2}$$

It ensues from the comparison of (1) and (2) that:

$$S_i^\varepsilon = S_i^\sigma \times \frac{\sigma}{\varepsilon^\%} = -S_i^\sigma \times \frac{E}{100} \tag{3}$$

Equation (3) supposes Young's Modulus E (in GPa) to be the same in compression and in tension, which we shall discuss further, on account of the bond nature and three-dimension-symmetry in silicon carbide structures. Note that E is the whole fiber Young's modulus, not that of the phase a mode of which is used for strain dependency determination. Calibrations of S_i^ε were done for carbon Raman contributions in polymeric, carbon and SiC fibers (refs. 18, 20 to 33). In the latter case, the results could be compared with S_i^ε of silicon carbide optical modes, which experienced different stress states in the two phases (ref. 4).

Theoretical predictions of strain-induced "Raman shifts" exist for cubic crystals (ref. 34) and the corundum structure (Ti$_2$O$_3$ (ref. 14) and α-Al$_2$O$_3$ (refs. 14 and 35). They are based on the elastic constants tensor and their use for the determination of biaxial stresses in layered materials like CVD diamond films (refs. 36 and 37) or locally oxidized silicon (LOCOS) (refs. 38 and 39) produced consistent results. The Grüneisen coefficient (ref. 40) is sometimes preferred to S_i^σ and S_i^ε to express the wavenumber sensitivity to external stresses. It is defined as a function of the volume (V) as:

$$\gamma_i = -\frac{\partial \log v_i}{\partial \log V} \tag{4}$$

If only the pressure component changing the unit cell parameters is considered (the so-called hydrostatic component, the other one changes bond angles (refs. 41 and 42)), then S_i^σ and γ_i are linked by a proportionality factor:

$$S_i^\sigma = \frac{v_i^0 \times \gamma_i}{B} \tag{5}$$

B is the material's bulk modulus $\left(B = -V \times \left(\frac{dP}{dV} \right)_T \right)$. In the general case, equations of state (EOS) linking V (or the cell parameters) to the applied stress are mandatory to correlate equations (1) and (4), in other words to compare S_i^σ and γ_i. Different EOS exist for solids, like Murnaghan's (refs. 9 and 43), the Birch-Murnaghan EOS (ref. 44) or Tait's EOS (ref. 45). Bridgeman also proposed a specific EOS for polymers (ref. 45). In cubic materials (V = a^3), γ_i can be obtained directly from the wavenumber shifts measured for an hydrostatic stress and shear stresses along high symmetry directions (refs. 12 and 13).

The Hi-Nicalon fiber consists of several phases, which are all somewhat amorphous. It would be unrealistic to theoretically predict strain-induced Raman shifts to them or to use reported Grüneisen coefficients. We will therefore use S_i^ε coefficients; however, the rather high measurement uncertainty necessitates the determination of optimum working conditions.

EXPERIMENTAL PROCEDURE

Samples and Equipment

The samples and the experimental equipment have been fully described in part 1 (ref. 1). The spectra were recorded on a "XY" spectrograph (Dilor, France) with a back-illuminated nitrogen-cooled CCD detector (Spex, France). The laser spot size could be lowered through a microscope from 100 to 300 μm ("Macro-configuration") to 1 μm ("Micro-configuration"). In the latter case, the beam could be scanned over the sample surface with the help of a mobile mirror. An "Ar-Kr" laser source (model "Innova 70" from Coherent, USA) allowed us to work with blue (457.9 and 488 nm), green (514.5 and 530.9 nm) and red (647.1 nm) excitations. A motorized X-Y displacement table was used for a two-dimensional-mapping of any given surface and the 556.3 nm line of a neon lamp that was installed in the spectrograph chamber was a wavenumber reference when working with the 514.5 nm laser line (the corresponding shift was 1460.4 cm^{-1}, peaking in the middle of carbon signal).

Our interest focused on three unidirectional celsian-matrix composites (12 plies), prepared by hot pressing of a calcined mixture of $BaCO_3$, $SrCO_3$, Al_2O_3 and SiO_2 powders. Composite No. 1 was reinforced by flame-desized Hi-Nicalon fibers (fiber volume fraction $V_f = 35$ percent), while composite No. 2 incorporated double-coated Hi-Nicalon fibers (a layer of ~0.4 μm pyrolytic BN (p-BN) overcoated by a ~0.2 to 0.3 μm thick SiC diffusion barrier; $V_f = 28$ percent). Composite No. 3 will refer to a composite similar to composite No. 2, but with a 12 wt % Si-doped p-BN layer (~0.4 μm thick) and an overcoating of SiC (~0.2 to 0.3 μm thick). Sections of each composite were polished perpendicular and parallel to the fiber direction. Some "reference" fibers were also extracted from composite No. 2 by matrix crushing in an agate mortar. Such extraction was impossible in composite No. 1 due to fiber strength degradation from mechanical damage during composite processing (ref. 46).

CHOICE OF THE "STRESS PROBE" AND FITTING PROCEDURE

Due to the high electronic absorption of C-C bonds in the visible-UV range, the symmetric stretching modes and their harmonics (pure or combined) are enhanced by a so-called "resonance" phenomenon (refs. 17 and 47). Hi-Nicalon "silicon carbide" fibers have a rather large excess of carbon (C:Si stoichiometric ratio of 1.4, that is 40 percent excess carbon), thus the signal C-C which will then be the most convenient "stress probe." Only in the nearly stoichiometric fibers, might the SiC spectrum be used for stress assessment. Our results will be based on the so-called "D band" whose attribution to "$C_{sp}{}^3 - C_{sp}{}^3/sp^2$" bonds has been discussed in part 1. "G band" ("sp^2"-like C-C bonds) has been preferred in fibers since the "sp^3" signal is either weak or less defined. In fact, the fine structure of the "sp^2" massif in the new generations of SiC fibers reveals a doublet, one component of which, D', has wavelength-dependent intensity and position (ref. 48). This component is only a shoulder in highly amorphous carbon, but is truly pronounced in SiC fibers. Besides, the doublet fitting depends to some extent on a smaller (but much wider) band, around 1530 cm^{-1} (carbon linked to heteroatoms (refs. 49 to 51)). Figure 1 illustrates typical decompositions performed using the Labspec software (Dilor, France). The first step is the systematic subtraction of a linear baseline attached to the spectral window limits. All known contributions are then entered close to their expected locations and are given a Gaussian shape, except for the "sp^3" carbon mode and the optical (TO/LO) modes of SiC, which are attributed to pure Lorentzian shapes. The adjusted parameters are the wavenumber (v), the full width at half height (w), the intensity, and the band area.

POWER AND WAVELENGTH-INDUCED MEASUREMENT DISTURBANCES

Thermal expansion has the same lengthening effect on bonds as tensile stress. Any localized heating induced by the laser impact might therefore lead one to overestimate tensile stresses and underestimate compressive ones. In unfavorable conditions, compression might even be confused with tensile stress. There is thus a need,

before stress analysis, for a preliminary study intended to assess the influence of working parameters on sample heating. The first parameter is the material itself (M), which includes the fiber composition and its environment; fibers are either free-standing in air, for S_i^ε calibrations, or embedded in a given matrix for in-situ measurements and a large influence of fiber surroundings on thermal dissipation is anticipated. The matrix should act as a huge heat sink and dissipate most of the accumulated heat (ref. 52). Other parameters that might have an effect on heating are the wavelength λ of the laser (because of carbon resonance), the laser power (P), the recording time (t) and the surface area impacted by the spot (A).

(i) Wavenumbers are highly sensitive to the power, which can be characterized by negative S_i^P parameters, in cm^{-1}/mW unit:

$$v_i = v_i^0 + S_i^p \times P \qquad (6)$$

Three examples of S_i^P measurement are given in figure 2, for $\lambda = 514.5$ nm. Results for nine tests corresponding to different conditions (fiber, setting, wavelength...) are shown in table I, with corresponding v_D^0 values. The eight tests on carbon D band measurements confirmed a linear mode softening with increasing power, for a variety of $\{t; A\}$ values. Regressions were extrapolated down to $P = 0$ mW although it looks like a very short dwell exists below 0.5 mW (although we can not rule out heating at such low powers). Only for SiC (TO mode) was a dwell clearly identified, up to 17 mW. Si-C bonds being non resonant in the visible range there is, therefore, no direct conversion of the photonic energy into heat. Heating is postponed and measurement confidence would probably be better using SiC as the stress probe (instead of the carbon signal) when new generations of nearly stoichiometric SiC fibers are studied, even if it means longer recording times. The carbon phase is so dispersed in nearly stoichiometric fibers that it no longer probes the actual stress anyway (ref. 4).

(ii) One expected result table I confirms is the poor dissipation ability of free-standing fibers, due to the low thermal conductivity of air. In contrast, the matrix surrounding a fiber in a composite acts as a heat sink, the dissipating effect being greater for a metallic matrix (Ti6242 alloy) than for ceramics (celsian).

(iii) The effect, if there is one, on changing A on the surface of free-standing fibers from 1 μm^2 (spot size) to 100 μm^2 (spot scanning by a mobile mirror) when $\{\lambda, P, t\}$ are set at given values remains below the statistical error.

(iv) If there is any "time effect" on heat accumulation, the equilibrium state must be reached very quickly. Indeed, we noticed wave numbers did not systematically decrease, at least for power below 10 mW, when t increased for a given set of $\{\lambda, M, A\}$.

Power clearly is the most important parameter. Data in table I will help us compensate the thermally induced Raman shift as a function of the sample and the wavelength used. Given the uncertainties, the maximal power per square micrometer that would not dramatically perturb the room temperature signal is about 1 mW for matrix-embedded fibers but falls, below 0.5 mW for free standing fibers.

RESULTS

Fiber Analysis

S_D^ε Calibration under axial tension.—A -2.7 (±0.4) $cm^{-1}/\%$ value has been obtained by Gouadec et al. (ref. 52) for S_D^ε in annealed Hi-Nicalon fibers (1000 °C in reducing atmosphere) observed with the $\lambda = 514.5$ nm line (table II caption in this reference wrongfully mentioned air annealing). Note that changing the power from 2 to 8 mW provoked a 9.1 cm^{-1} shift of v_D, which agrees well with the 9.2 cm^{-1} shift predicted on the basis of table I. In addition, S_D^ε measurement showed a good reproducibility for fibers analyzed under equivalent conditions, which was not true for S_G^ε. Hence the "stress-sensitivity" of the D band is greater than that of G. Figure 3(a) shows that for a pure carbon fiber (FT700 grade), both v_D and S_D^ε change linearly with the exciting laser line energy. A similar linear behavior is found for v_D in Hi-Nicalon fibers (fig. 3(b)) and can consequently be expected also for their S_D^ε.

In situ Results; Comparison with stress-free references.—Once S_i^ε is known, it becomes possible to interpret wavenumber shifts from one place to another in terms of stress difference. The actual loading at each point requires a v_i^0 "stress-free" reference measured at room temperature. v_i^0 might unfortunately differ from one sample to another and a value found in the sample itself is expected to be the most reliable possible, at least more than that obtained from S_i^ε calibrations. Besides, measuring the stress in the same sample as the reference would avoid compensating for the "laser heating" issue. The two spectra of the longitudinal mapping of figure 4 (458 nm) that were recorded on the fiber crack in composite No. 2 are almost stress-free internal references. With 5 mW exciting power, their D band mean

wavenumber was 1358.80 (±1.00) cm^{-1}, the mean for all other probed points being 1365.75 (±0.15) cm^{-1}. There is thus strong evidence that the fiber is in compression in the matrix. The fitting of spectra that were recorded under the very same conditions on cross sections gave an average 1366.20 (±0.30) cm^{-1} wavenumber (7 measurement points). Some matrix being removed on polished cross sections, one might expect greater stress effects on spectra recorded through the matrix. Such recording was not possible, due to celsian's low transparency ($\leq$20 μm). But, Wu and Colomban found equivalent results for fiber reinforced mullite probed on cross sections and through the matrix (ref. 53). This peculiar behavior must result from CMCs having reloading lengths of a few microns only, much smaller than the typical 500 to 1000 μm values encountered in organic matrix composites (ref. 19).

Cross-sectional probing performed with 2 mW power (instead of 5 mW) produced a value of ~1367.20 ± 0.25 cm^{-1} (100 s/spectrum). According to figure 2, a 0.7 cm^{-1} heating-induced shift is anticipated when power is changed from 2 to 5 mW. The results are therefore consistent, provided the preliminary study on power influence is taken into account.

All shifts we measured on composites Nos. 1 and 2 remained low compared with the experimental accuracy and we decided to record additional series of spectra with the 514.5 nm wavelength, for the neon line to be systematically included as a reference (ref. 52). Besides, this wavelength allows carbon signal recording at once (one window only, hence better fitting) and we already had a S^{ϵ}_{D} value. The power was fixed at 1 mW on the sample, the lowest possible value still giving acceptable spectra quality for reasonable recording times. We retained 180 sec/spectrum, but we checked that a 900 sec recording did not produce different values, neither for wavenumbers, nor for bandwidths.

The in situ results are presented in figure 5. Spectra were recorded on cross sectional views (on polished composites), freshly cut fiber sections or sections of extracted fibers; the latter constitute an internal reference. Different regions were tested in composites Nos. 1 and 2 for statistical analysis. Plotted values are average with error bars indicating the extremes. Figure 6 gives an example of a two-dimensional mapping performed on composite No. 1 under the conditions used for figure 5. Again, a correction of the apparatus shift was done using the neon line as a reference.

Interphase Materials

SiC and Si spectra were presented in part 1 (ref. 1) from a qualitative point of view. The wavenumbers will be discussed below in terms of possible strains, which will not be possible for BN, due to a disturbing signal scattering phenomenon (ref. 1).

DISCUSSION

The Fiber Stress in the Composites

The above-mentioned apparent compression is in perfect agreement with the coefficient of thermal expansion (CTE) of the Hi-Nicalon fiber ($\alpha = 3.5 \times 10^{-6}/°C$ between room temperature (RT) and 500 °C, from Nippon carbon data sheets) and the celsian matrix ($\alpha = 5.28 \times 10^{-6}/°C$ between RT and 1200 °C (ref. 54)). For CMCs, the reinforcement CTE should be greater, to put the matrix, whose tensile strength is low, under residual compression and, in this way, prevent microcracking up to acceptable loading (ref. 55). Yet, low α materials usually have loosely packed frameworks and a compromise must be found to keep acceptable mechanical properties. The best matrix choice requires a chemical and mechanical analysis of the multiphase materials. Note that α of monoclinic celsian phase of $SrAl_2Si_2O_8$ was measured to be $2.5 \times 10^{-6}/°C$ by Bansal (ref. 56), which confirms thermal expansion of celsian is a function of the alkali/alkaline-earth content (ref. 57).

Anticipated Stress.—According to Wu et al. (ref. 58), the axial (σ_A) and transverse (σ_T) residual stresses in an "infinite" fiber, that is to say a long and nonfragmented fiber, embedded in a given matrix, can be calculated using the following expressions:

$$\sigma_A = \frac{\left[\frac{2\nu_A}{E_A}(\alpha_T - \alpha_m) + \left(\frac{1-\nu_T}{E_T} + \frac{1+\nu_m}{E_m} \right)(\alpha_A - \alpha_m) \right] E_A \times \Delta T}{\left(\frac{2\nu_A^2}{E_A} - \frac{1-\nu_T}{E_T} - \frac{1+\nu_m}{E_m} \right)} \quad (7)$$

$$\sigma_T = \frac{\left[\alpha_T - \alpha_m + \nu_A(\alpha_A - \alpha_m)\right] \times \Delta T}{\left(\dfrac{2\nu_A^2}{E_A} - \dfrac{1-\nu_T}{E_T} - \dfrac{1+\nu_m}{E_m}\right)} \qquad (8)$$

The subscripts in equations (7) and (8) are relative to the matrix (m) and the axial (A) or transverse (T) properties of the fiber. ν are Poisson ratios and ΔT represents the difference between room temperature (RT) and the so-called "induction temperature," T_i, at which the matrix becomes too "soft" to constrain the fiber (ref. 59) (see above for significance of E and α). Due to lack of availability of experimental values of T_i, we will replace it by $T_S = 1300$ °C, a typical sintering temperature for alumino-silicate matrices. Besides, given the relative isotropy of Hi-Nicalon fibers and, again, due to lack of data, axial and transverse properties should be considered the same (with a subscript f). If we now put all Poisson ratios to zero, which is partly justified as a first approximation by the very local probing scale of Raman spectroscopy, equations (7) and (8) simplify to:

$$\sigma_a = (\alpha_m - \alpha_f) \times \Delta T \times E_f \qquad (9)$$

$$\sigma_a = (\alpha_m - \alpha_f) \times \Delta T \times \frac{(E_m E_f)}{(E_m + E_f)} \qquad (10)$$

Taking $E_m = 96$ GPa (ref. 54) and assuming the $E_f = 270$ GPa Young's modulus given by Nippon Carbon Company for Hi-Nicalon fibers, the compressive stress should be about 600 to 650 MPa, axially, and >150 MPa, radially. The stress measurement derived from (unpolarised) Raman spectra should fall in between since the method is not sensitive to the loading direction, at least in amorphous materials.

Experimental Stress Assessment.—Looking at figure 5, the wavenumbers of the Hi-Nicalon fibers before matrix embedding are rather close: uncoated and coated fibers are suitable to serve as "stress-free" references. Their bandwidths are slightly different, but figure 7 in part 1 showed structural evolution of Hi-Nicalon fibers begins around 1300 to 1400 °C, which happens to be the temperature range of p-BN/SiC chemical vapor deposition.

The experimental wavenumber shift $\Delta \nu_{Exp}^D$ of D band of any Hi-Nicalon fiber, measured with respect to the "stress free reference" of a free-standing fiber ($\nu_{Free\text{-}standing}$) has three possible origins. It can result from a mechanical stress ($\Delta \nu_{stress}$), but laser heating ($\Delta \nu_{Heating}$) and/or chemical alterations ($\Delta \nu_{Chemistry}$) must also be considered:

$$\Delta \nu_{Exp}^D = \nu_{Sample} - \nu_{Free\text{-}standing} = \Delta \nu_{Stress} + \Delta \nu_{Heating} + \Delta \nu_{Chemistry} \qquad (11)$$

The stress-related shift, the one we want to know, is given by equation (2):

$$\Delta \nu_{Stress} = S_{Hi\text{-}Nicalon}^{\varepsilon} \times \Delta \varepsilon^{\%} \qquad (12)$$

Concerning the laser heating, it is straightforward to write:

$$\Delta \nu_{Heating} = P \times \left(S_{sample}^{P} - S_{Free\text{-}standing}^{P}\right) \qquad (13)$$

As for the chemical term, it can be neglected in our case, on account of the small bandwidth difference between embedded and reference fibers. This approximation is ascertained by the fact that $\Delta \nu_{Exp}^D \cong 0$ for the fiber extracted from composite No. 2 (it has the same wavenumber in figure 5 as the "stress-free" references of the left hand side), for which $\Delta \nu_{Stress}$ and $\Delta \nu_{Heating}$ must vanish. All in all, the residual compressive stress will be obtained from the following expression:

$$\Delta \sigma = -E_f \times \Delta \varepsilon = -\frac{E_f}{100} \times \Delta \varepsilon^{\%} = -\frac{E_f}{100} \times \frac{\Delta \nu_{Stress}}{S_{Hi\text{-}Nicalon}^{\varepsilon}} = \frac{E_f \times \left(P \times S_{sample}^{P} - P \times S_{Free\text{-}standing}^{P} - \Delta \nu_{Exp}^D\right)}{100 \times S_{Hi\text{-}Nicalon}^{\varepsilon}} \qquad (14)$$

After figure 5, for which P is 1 mW, the experimental shifts are the following:

$$\Delta v_{Exp}^{\#1} = \Delta v_{Exp}^{\#3} = 1353.65 - 1351.70 = 1.95 \text{ cm}^{-1}$$

$$\Delta v_{Exp}^{\#2} = 1352.80 - 1351.70 = 1.10 \text{ cm}^{-1}$$

If we put these shifts in equation (14), taking $E_f = 270$ GPa; $S_{Hi-Nicalon}^{\varepsilon} = -2.7 \text{ cm}^{-1}/\%$; $S_{D \text{ in celsian}}^{P/514.5 \text{ nm}} = -0.55 \text{ cm}^{-1}/\text{mW}$ and $S_{D \text{ Freestanding}}^{P/514.5 \text{ nm}} = -1.54 \text{ cm}^{-1}/\text{mW}$, the calculated stress is 110 MPa compression in composite No. 2 ; a 960MPa compression in composites Nos. 1 and 3. Hence, the p-BN/SiC interphase apparently relaxes the residual stress, but not the silicon-doped one. Besides, working with the 514.5 nm line, we found that v_D in a fiber surrounded by a preserved p-BN/SiC double coating was lower than in a nearby fiber with a broken SiC ring, where p-BN layer had dissolved in the celsian. The BN layer acts as a compliant material which protects the fibers and results in better σ_r and m (Weibull modulus) values in the composite (refs. 60 and 61).

The compressive stresses we found (100 and 950 MPa) are not exactly in the range anticipated from our micromechanical modeling (150 to 650 MPa). Yet, the estimate relied on many approximations and did not consider interphase materials at all. On the other hand, the values of S_D^P that we used for the Raman measurement might not be the exact ones. Besides, we possibly incorrectly estimated the value of S_i^{ε}. Indeed, measurements on carbon (ref. 30) and polymeric fibers (ref. 32) revealed a slight but steady softening when stresses were changed from tensile to compressive ($E_{tensile} > E_{compression}$). Despite this phenomenon, equation (1) remained valid, which, according to equation (6), meant a correlative decrease of S_i^{ε} in compression. Wavenumber shifts were no longer proportional to the strain (ref. 21) and equation (2) had to be replaced by second or even third order polynomial expressions (P75 (ref. 26) and Graphil XAS (ref. 31) carbon fibers) to unify compressive and tensile behaviors for first and second order bands. However, ceramics consist of highly covalent bonds, have a three-dimensional-structure and no failure initiating defects in compression. Besides, in the peculiar case of the Hi-Nicalon fibers, there is a uniform distribution of C and SiC species, Si-C bonds have a high strength and SiC grains have no boundary since excess carbon just substitutes for Si atoms. We therefore assume our S_D^{ε} value is almost the same whatever the sign of the applied strain, at least in the explored range. Hi-Nicalon fibers dependency must remain linear, as was shown for fully crystalline polydiacetylene fibers (ref. 21).

Statistical Relevance of the Results.—It must be pointed out that not only the recording conditions, but also the statistical dispersion between the fibers (batch, size, coating, environment...) must be taken into account to ascertain the effect of chemical degradation or stress concentration on the Raman spectra. For instance, core wavenumbers in figures 5 and 6 differ in spite of perfectly identical working conditions. Yet, there is good consistency in the series of experiments we carried on composites Nos. 1 and 2 (fig. 5). The extreme values we obtained on nine different fibers of the same part of a sample and for the same recording conditions (488 nm) were ~1359.5 and 1360.3 cm⁻¹. A tenth fiber, isolated from the others by at least ten diameters showed a higher value of ~1360.7 cm⁻¹. Thus, the compression would be attenuated by the presence of surrounding fibers, which would mean, as expected, that the matrix plays a more important role than the interphase in compressing the fibers.

Possible Edge Effect.—Figures 6(b) shows evidence of an apparent stress relaxation about 3 μm from the fiber-matrix interphase in composite No. 1. A band widening is observed at the very interface in figure 6(c), which suggests a chemical alteration (or fitting errors due to intensity lowering), but the wavenumber shift must have a mechanical effect for the region of constant bandwidth. The best way to ascertain why the C-C bonds of the edge region are different would be to record spectra on nickel-embedded fibers, which would rule out any mechanical effect (ref. 62). A small "compression relaxation" was detected in composite No. 2 when moving away from the fiber core, but no proper "edge analysis" could be performed where BN contribution was affecting the bandwidths.

Wavelength influence.—Rapid mappings performed with four different wavelengths (458/488/514/647 nm) confirmed the compressive nature of the stress in composite No. 2, but with a constant difference, about 1 cm⁻¹, between "stress-free" references (either desized fibers or extracted fibers) and the wavenumber measured in situ. If S_D^{ε} really depends linearly on the laser energy (in eV unit), according to figure 3 comments above, then we must conclude that the stress is wavelength-dependant. As a matter of fact, light penetration in resonant materials is correlated with the wavelength. Assuming that the absorption of Hi-Nicalon fibers should be close to that of amorphous silicon carbide (a-SiC) films, which is ascertained by Raman spectra similitude, the maximal penetrations can be assumed to be about 25 and 75 nm for the 458 and 647.1 nm lines, respectively (ref. 63). There might exist actual stress differences as a function of the distance to the sample surface or, in other words, the analyzed volume. Our observation would indicate a stress gradient with the lowest stress measured at the very surface of the sample (blue laser observation). This seems logical, but more detailed results would require precise measurements of the laser power and using reference lamps for red and blue excitations.

OVERCOATING ANALYSIS

For SiC and Si materials, the only values at our disposal were found in the literature for compressive experiments in diamond anvils on single crystal pieces. The sensitivity of SiC spectra to pressure has been investigated with the 514.5 nm line for the 3C (refs. 43 and 64), 6H (refs. 8, 64 and 65) and 15R (ref. 64) polytypes. Linear dependencies of 3.53 ± 0.21 and 4.28 ± 0.22 cm^{-1}/GPa were calculated respectively for the TO and LO modes of 6H-SiC (ref. 8), which our SiC layer mainly consists of (see part 1). TO$_1$ and LO modes are at their expected values (796 and 966 cm^{-1}, respectively) but TO$_2$ mode points at 788 cm^{-1}, while its reported stress-free value is about 789.2 cm^{-1}. This would correspond to a huge stress, but this "shift attribution" would be dubious and the great variety of recorded spectra (see part 1) is rather a consequence of great structural variations (SiC polytypism, see part 1).

Apparently, the more intense the silicon signal, the weaker the TO$_1$ contribution. Silicon unsplit (stress-free) wavenumber peaks at 520.6 cm^{-1} (ref. 66). It is a triply degenerate mode where stress-induced splitting has been fully reported in the literature along the [111] and [001] directions (ref. 13), or biaxial strains in a polycrystalline silicon thin layer (refs. 66 and 67). The mean value (weighted by the degeneracy) must be considered in disordered silicon and the splitting explains band widening observed in strained silicon. In our samples we detected a mean 2 cm^{-1} shift, which would indicate compressive stresses of about 1 GPa (the mean sensitivity is 500 MPa/cm^{-1} (ref. 68)). Such value would be very high for a macroscopic stress, but what is measured here is a very local stress.

SUMMARY

The fibers are under compressive residual stress of 950 MPa in celsian matrix composites reinforced with uncoated or p-B(Si)N/SiC coated Hi-Nicalon fibers. In another celsian matrix composite, where Hi-Nicalon fibers have been coated with undoped p-BN/SiC, residual stress in the fibers seems to have significantly relaxed to 110 MPa. In addition, the compression seems to reach a higher level at the fiber core than in the vicinity of the fiber-matrix interface. More precise results would require (i) taking into account the effective Young's Modulus in compression, (ii) performing calibrations under compression, and (iii) using fibers annealed under the conditions of composite fabrication as a reference.

CONCLUSION

For Hi-Nicalon fiber-reinforced composites, a stress relaxation-like phenomenon was observed at the surface of p-BN/SiC-coated Hi-Nicalon fibers whereas the uncoated or p-B(Si)N/SiC-coated fibers did not show any stress relaxation. This is presumably due to différences in the compliance of the two interphase coatings.

REFERENCES

1. G. Gouadec, Ph. Colomban and N.P. Bansal: "Raman Study of Uncoated and p-BN/SiC-Coated Hi-Nicalon Fiber Reinforced Celsian Matrix Composites, Part 1: Distribution and Nanostructure of Different Phases," NASA/TM—2000-210340, Aug 2000, J. Am. Ceram. Soc.
2. Ph. Colomban and J. Corset: J. Raman. Spectrosc., 30 [10], pp. 861–947 (1999) - "Special Issue on Raman (Micro) Spectrometry and Materials Science."
3. M.A. White: "Thermal Properties of Solids: Etude in Three-part Anharmony," Can. J. of Chem., 74, pp. 1916–1921 (1996).
4. G. Gouadec and Ph. Colomban: "Raman Extensometry: Anharmonicity and Stress;" pp. 759–766 in Proceedings of 11èmes Journées Nationales sur les Composites (JNC11)-Arcachon, France, Nov 18–20 (1998).
5. M. Hanfland, K. Syassen, S. Fahy, S.G. Louie and M.L. Cohen: "Pressure Dependence of the First-Order Raman Mode in Diamond," Phys. Rev., B31 [10], pp. 6896–6899 (1985).
6. S.-J. Jeon, D. Kim, S.K. Kim and I.C. Jeon: "High-Pressure Raman Study of Fullerite C60," J. Raman Spectrosc., 23, pp. 311–313 (1992).
7. S.H. Tolbert, A.P. Alivisatos, H.E. Lorenzana, M.B. Kruger and R. Jeanloz: "Raman Studies on C60 at High Pressures and Low Temperatures," Chem. Phys. Lett., 188 [3,4], pp. 163–167 (1992).

8. J.F. DiGregorio and T.E. Furtak: "Analysis of Residual Stress in 6H-SiC Particles within Al_2O_3/SiC Composites Through Raman Spectroscopy," J. Am. Ceram. Soc., 75 [7], pp. 1854–57 (1992).

9. G. Salvador and W.F. Sherman: "Pressure Dependence of the Raman Phonon Spectrum in 6H-Silicon Carbide," J. Molec. Struct., 247, pp. 373–384 (1991).

10. B. Reynard and D.C. Rubie: "High-Pressure, High-Temperature Raman Spectroscopic Study of Ilmenite-Type $MgSiO_3$," Am. Miner., 81, pp. 1092–1096 (1996).

11. L.-G. Liu and T.P. Mernagh: "Phase Transitions and Raman Spectra of Anatase and Rutile at High Pressures and Room Temperature," Eur. J. Miner., 4, pp. 45–52 (1992).

12. M.H. Grimsditch, E. Anastassakis and M. Cardona: "Effect of Uniaxial Stress on the Zone-Center Optical Phonon of Diamond," Phys. Rev., B18 [2], pp. 901–904 (1978).

13. E. Anastassakis, A. Pinczuk, E. Burnstein, F.H. Pollak and M. Cardona: "Effect of Static Uniaxial Stress on the Raman Spectrum of Silicon," Solid State Comm., 8, pp. 133–138 (1970).

14. S.H. Shin, F.H. Pollak and P.M. Raccah: "Effects of Uniaxial Stress on the Raman Frequencies of Ti_2O_3 and Al_2O_3," in Light scattering in solids, pp. 401–405 (1975).

15. S. Venugopalan and A. Ramdas: "Effect of Uniaxial Stress on the Raman Spectra of Cubic Crystals: CaF_2, BaF_2, and $Bi_{12}GeO_{20}$," Phys. Rev., B8 [2], pp. 717–734 (1973).

16. T.A. Michalske, D. Tallant and W.L. Smith: "Raman Study of Silica Glass Under Tensile Stress," Phys. Chem. of Glasses, 29 [4], (1988).

17. Ph. Colomban: "Raman Microspectrometry and Imaging of Ceramic Fibers in CMCs and MMCs," in Advances in Ceramic Matrix Composites V, N.P. Bansal, J.P. Singh and E. Ustundag, Editors; Am. Ceram. Soc. (Westerville, OH, U.S.A), Ceram. Trans., 103, pp. 517–540 (2000).

18. R.J. Young: "Analysis of Composites Using Raman and Fluorescence Microscopy–a Review," J. Microscopy, 185 [2], pp. 199–205 (1996).

19. M.S. Amer and L.S. Schadler: "The Effect of Interphase Toughness on Fiber/Fiber Interaction in Graphite/Epoxy Composites: An Experimental and Modeling Study," J. Raman Spectrosc., 30 [10], pp. 919–928 (1999).

20. C. Galiotis, A. Paipetis and C. Marston: "Unification of Fiber/Matrix Interfacial Measurements with Raman Microscopy," J. Raman. Spectrosc., 30 [10], pp. 899–912 (1999).

21. L.S. Schadler and C. Galiotis: "Fundamentals and Applications of Micro Raman Spectroscopy to Strain Measurements in Fiber Reinforced Composites," Inter. Mater. Rev., 40 [3], pp. 116–134 (1995).

22. M.C. Andrews and R.J. Young: "Analysis of the Deformation of Aramid Fibers and Composites Using Raman Spectroscopy," J. Raman Spectrosc., 24, pp. 539–544 (1993).

23. I.J. Beyerlein, M.S. Amer, L.S. Schadler and S.L. Phoenix: "New Methodology for Determining in-situ Fiber, Matrix and Interfaces Stresses in Damaged Multifiber Composites," Sci. Eng. Comp. Mater., 151, 204 (1998).

24. K.D. Cowley and P.W.R. Beaumont, "The Measurement and Prediction of Residual Stresses in Carbon-Fiber/Polymer Composites," Comp. Sci. Techn., 57, pp. 1445–1455 (1997).

25. R.J. Day, I.M. Robinson, M. Zakikhani and R.J. Young: "Raman Spectroscopy of Stressed High Modulus Poly (p-phenylene benzobisthiazole) Fibers," Polymer, 28, pp. 1833–1840 (1987).

26. C. Filiou, C. Galiotis and D.N. Batchelder: "Residual Stress Distribution in Carbon Fiber/Thermoplastic Matrix Pre-Impregnated Composite Tapes," Composites, 23 [1], pp. 28–38 (1992).

27. G. Gouadec and Ph. Colomban: "Micro-Raman Stress Imaging of Ceramic (C, SiC) Fiber-Reinforced CMCs and MMCs," Mater. Sci. Eng. A, (2000).

28. P.W.J. Van Den Heuvel, T. Peijs and R.J. Young: "Failure Phenomena in Two-Dimensional Multi-Fiber Microcomposites. Part 2: A Raman Spectroscopic Study of the Influence of Inter-Fiber Spacing on Stress Concentrations," Comp. Sci. Techn., 57 [8], pp. 899–911 (1997).

29. D. Lévêque and M.H. Auvray: "Study of Carbon Fibers Strain in Model Composites by Raman Spectroscopy," pp. 599–608 in Proceedings of 9èmes Journées Nationales sur les Composites (JNC9)-Saint-Etienne, Nov 22–24 (1994).

30. N. Melanitis and C. Galiotis: "Compressional Behavior of Carbon Fibers. Part 1: a Raman Spectroscopy Study," J. Mater. Sci., 25 [12], pp. 5081–5090 (1990).

31. N. Melanitis, P.L. Tetlow, C. Galiotis and S.B. Smith: "Compressional Behavior of Carbon Fibers, Part II: Modulus Softening," J. Mater. Sci., 29, pp. 786–799 (1994).

32. C. Vlattas and C. Galiotis: "Monitoring the Behavior of Polymer Fibers Under Axial Compression," Polymer, 32 [10], pp. 1788–1793 (1991).

33. C. Galiotis: "Laser Raman Spectroscopy, a New Stress/Strain Measurement Technique for the Remote and On-line Nondestructive Inspection of Fiber Reinforced Polymer Composites," Mater. Techn., 8 [9/10], pp. 203–209 (1993).

34. E. Anastassakis: "Selection Rules of Raman Scattering by Optical Phonons in Strained Cubic Crystals," J. Appl. Phys., 82 [4], pp. 1582–1591 (1997).

35. W. Jia and W.M. Yen: "Raman Scattering From Sapphire Fibers," J. Raman Spectrosc., 20, pp. 785–788 (1989).

36. J.W. Ager III and M.D. Drory: "Quantitative Measurement of Residual Biaxial Stress by Raman Spectroscopy in Diamond Grown on a Ti Alloy by Chemical Vapor Deposition," Phys. Rev., B48 [4], pp. 2601–2607 (1993).

37. Y.V. Kaenal, J. Stiegler, J. Michler and E. Blank: "Stress Distribution in Heteroepitaxial Chemical Vapor Deposited Diamond Films," J. Appl. Phys., 81 [4], pp. 1726–1736 (1997).

38. I. De Wolf, J. Vanhellemont, A. Romano-Rodriguez, H. Norstrom and H.E. Maes: "Micro-Raman Study of Stress Distribution in Local Isolation Structures and Correlation with Transmission Electron Microscopy," J. Appl. Phys., 71 [2], pp. 898–906 (1992).

39. I. De Wolf: "Stress Measurements in Si Microelectronics Devices using Raman Spectroscopy," J. Raman Spectrosc., 30 [10], pp. 877–883 (1999).

40. E. Grüneisen: "Theorie des Festen Zustandes Ernatomiger Elemente," Annal. Physik, 39 pp. 257–306 (1912).

41. H. Mohrbacher, K.V. Acker, B. Blanpain, P.V. Houtte and J.-P. Celis: "Comparative Measurement of Residual Stress in Diamond Coatings by Low-Incident-Beam-Angle-Diffraction and Micro-Raman Spectroscopy," J. Mater. Res., 11 [7], pp. 1776–1782 (1996).

42. J.G. Kim and J. Yu: "A Study on the Residual Stress Measurements Methods on Chemical Vapor Deposition Diamond Films," J. Mater. Res., 13 [11], pp. 3027–3033 (1998).

43. D. Olego, M. Cardona and P. Vogl: "Pressure Dependence of the Optical Phonons and Transverse Effective Charge in 3C-SiC," Phys. Rev., B25 [6], pp. 3878–3888 (1982).

44. T.P. Mernagh, L.-G. Liu and C.-C. Lin: "Raman Spectra of Chondrodite at Various Temperatures," J. Raman Spectrosc., 30, pp. 963–969 (1999).

45. J.J. Flores and E.L. Chronister: "Pressure-Dependant Raman Shifts of Molecular Vibrations in Poly(methyl methacrylate) and Polycarbonate Polymers," J. Raman. Spectrosc., 27, pp. 149–153 (1996).

46. N.P. Bansal and J.I. Eldridge: "Hi-Nicalon Fiber-Reinforced Celsian Matrix Composites: Influence of Interface Modification," J. Mater. Res., 13 [6], pp. 1530–1537 (1998).

47. W. Kiefer and M. Spiekermann: "Applications of Non-Classical Raman Spectroscopy: Resonance Raman, Surface Enhanced Raman, and Nonlinear Coherent Raman Spectroscopy," in Infrared and Raman Spectroscopy. Methods and Applications, B. Schrader Editor, VCH (Weinheim), pp. 465–517 (1995).

48. G. Gouadec, J.-P. Forgerit, H. Mendil, K. Devivier and Ph. Colomban: "Extensométrie Raman de Fibres C et SiC: Choix des Conditions par Corrélation 2D (Raman Extensometry of C and SiC Fibers: Conditions Choice by "2D Correlation);" in Proceedings of JNC12 (2000).

49. M. Ramsteiner and J. Wagner: "Resonant Raman Scattering of Hydrogenated Amorphous Carbon: Evidence for p-Bonded Carbon Clusters," Appl. Phys. Lett., 51 [17], pp. 1355–1357 (1987).

50. F. Mauri and A.D. Corso: "Vibrational Properties of Tetrahedral Amorphous Carbon From First Principles," Appl. Phys. Lett., 75 [5], pp. 644–646 (1999).

51. M. Yoshikawa, N. Nagai, M. Matsuki, H. Fukuda, G. Katagiri, H. Ishida, A. Ishitani and I. Nagai: "Raman Scattering from sp^2 Carbon Clusters.," Phys. Rev., B46 [11], pp. 7169–7174 (1992).

52. G. Gouadec, S. Karlin and Ph. Colomban: "Raman Extensometry Study of NLM202 and Hi-Nicalon SiC Fibers," Composites, 29B, pp. 251–261 (1998).

53. J. Wu and Ph. Colomban: "Raman Spectroscopy Study on the Stress Distribution in the Continuous Fiber-Reinforced CMC," J. Raman Spectrosc., 28, pp. 523–529 (1997).

54. N.P. Bansal: "Solid State Synthesis and Properties of Monoclinic Celsian," J. Mater. Sci., 33 [19], pp. 4711–4715 (1998).

55. T. Scanu, J. Guglielmi and Ph. Colomban: "Ion Exchange and Hot Corrosion of Ceramic Composites Matrices: a Vibrational and Microstructural Study," Solid State Ionics, 70/71, pp. 109–120 (1994).

56. N.P. Bansal: "Influence of Fiber Volume Fraction on Mechanical Behavior of CVD SiC Fiber/$SrAl_2Si_2O_8$ Glass-Ceramic Matrix Composites," J. Adv. Mater., 28 [1], pp. 48–58 (1996).

57. Ph. Colomban, H. Courret, F. Romain, G. Gouadec and D. Michel: "Sol-Gel Prepared Pure and Li-Doped Hexacelsian Polymorphs: An IR, Raman and Thermal Expansion Study of the b Phase Stabilization by Frozen Short-Range Disorder," J. Am. Ceram. Soc (To be published).

58. W. Wu, M. Desaeger, I. Verpoest and J. Varna: "An Improved Analysis of the Stresses in a Single-Fibre Fragmentation Test: I. Two-Phase Model," Comp. Sci. Techn., 57, pp. 809–819 (1997).

59. J.R. Wood, Y. Huang, R.J. Young and G. Marom: "Measurement of Thermal Strains During Compressive Fragmentation in Single-Fiber Composites by Raman Spectroscopy," Comp. Sci. Techn., 55, pp. 223–229 (1995).

60. N.P. Bansal: "Tensile Strength and Microstructure of Hi-Nicalon Fibers Extracted from Celsian Matrix Composites," in Advances in Ceramic Matrix Composites IV, J.P. Singh and N.P. Bansal, Editors: Am. Ceram. Soc. (Westerville, OH, U.S.A.), Ceram. Trans., 96, pp. 3–16 (1999).

61. N.P. Bansal: "Effects of HF Treatments on Tensile Strength of Hi-Nicalon Fibers," J. Mater. Sci., 33, pp. 4287–4295 (1998).

62. G. Gouadec and Ph. Colomban: "De l'Analyse Micro/Nano-Structurale et Micromécanique à l'Imagerie des Fibres de Renfort d'un Composite à Matrice Métallique (From Micro/Nano -Structure and -Mechanical Analysis to Imaging of Fibers Reinforcing a MMC)," J. Phys. IV, Pr4, 10, pp. 69–74 (2000).

63. G. Derst, C. Wilbertz, K.L. Bhatia, W. Krätschmer and S. Kalbitzer: "Optical Properties of SiC for Crystalline/ Amorphous Pattern Fabrication," Appl. Phys. Lett., 54 [18], pp. 1722–1724 (1989).

64. I.V. Aleksandrov, A.F. Goncharov, E.V. Yakovenko and S.M. Stishov: "High Pressure Study of Diamond, Graphite and Related Materials," in High-Pressure Research: Application to Earth and Planetary Sciences, Y. Syono and M.H. Manghnani Editors; Terra Scientific Publishing Company (TERRAPUB), Tokyo-Am. Geophysical Union, Washington D.C., pp. 409–416 (1992).

65. J. Liu and Y.K. Vohra: "Raman Modes of 6H Polytype of Silicon Carbide to Ultrahigh Pressures: A Comparison with Silicon and Diamond," Phys. Rev. Lett., 72 [26], pp. 4105–4108 (1994).

66. Y.M. Cheong, H.L. Marcus and F. Adar: "Raman Microprobe Measurements of Residual Strains at the Interfaces of Si on Quartz," J. Mater. Res., 2 [6], pp. 902–909 (1987).

67. M. Holtz, J.C. Carty and W.M. Duncan: "Ultraviolet Raman Stress Mapping in Silicon," Appl. Phys. Lett., 74 [14], pp. 2008–2010 (1999).

68. I. De Wolf, H.E. Maes and S.K. Jones: J. Appl. Phys., 79, pp. 7149 (1996).

69. X.J. Ning and P. Pirouz: "The Microstructure of SCS-6 SiC Fiber," J. Mater. Res., 6 [10], pp. 2234–2248 (1991).

TABLE I.—ORDINATE AT ORIGIN v_i^0 AND SLOPE S^p_i OF LINEAR REGRESSIONS CALCULATED AFTER THE FITTED WAVENUMBERS OF MODE i, PLOTTED AS A FUNCTION OF THE LASER POWER P (in mW, MEASURED ON THE SAMPLE). FT700 IS A PURE CARBON FIBER (TONEN, JAPAN); SCS6 FIBER (TEXTRON, U.S.A.) IS A 33 μm DIAMETER CARBON FILAMENT SURROUNDED BY A 50 μm THICK SIC LAYER (ref. 69).

Mode i/Fiber/Matrix/λ(nm)	v_i^0 (cm^{-1})	S^p_i (cm^{-1}/mW)
Carbon D band/Hi-S Nicalon/[a]/647.1	1326.11	–1.30
"D"/Hi-Nicalon/[a]/514.5	1353.96	–1.54
"D"/Hi-Nicalon[b]/[a]/514.5	1357.76	–1.60
"D"/FT700/ - /514.5	1354.18	–0.20
"D"/SCS6/Ti alloy/514.5	1354.26	–0.47
"D"/Hi-Nicalon/celsian/514.5	1355.06	–0.55
"D"/Hi-Nicalon/celsian/457.9	1368.90	–0.70
"D"/Hi-Nicalon/celsian/647.1	1328.88	–0.57
SiC to mode[d]/SCS6(SiC)/Ti alloy/514.5	791.49	0[c]

[a]Free-standing fiber.
[b]Scanning over 100 μm.
[c]In the center of carbon filament.
[d]12.5 μm from the fiber edge.
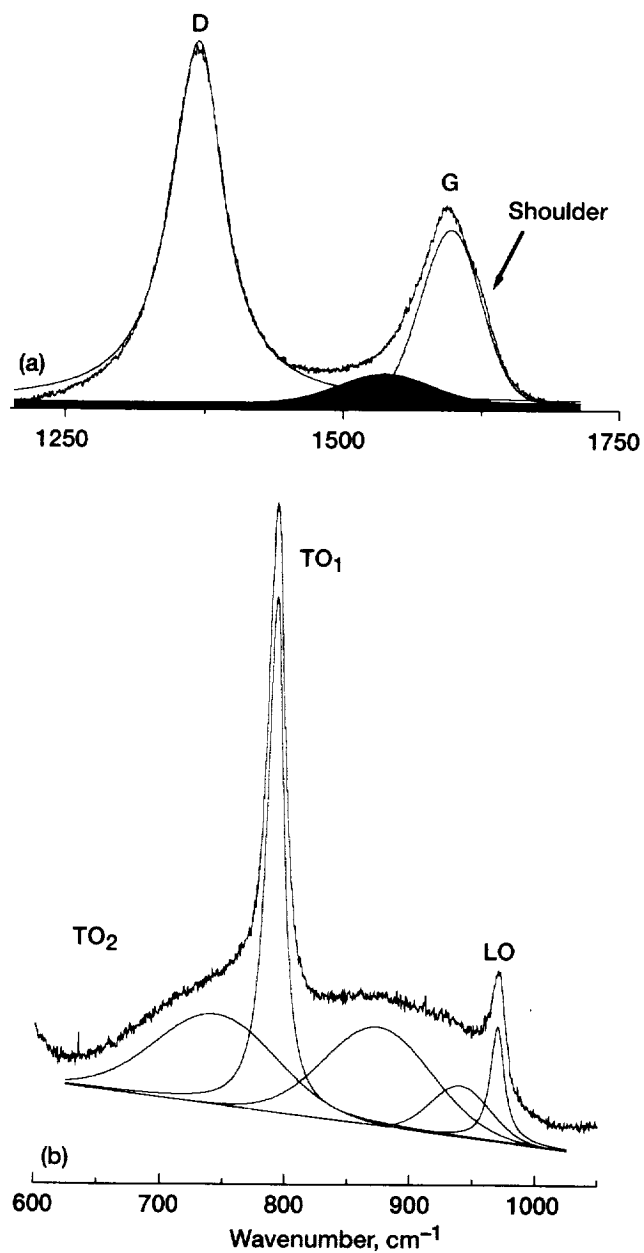[e] $S^P_{TO-SiC} = -0.07$ cm^{-1}/mW for P > 17mW.

Figure 1.—Typical examples of spectral deconvolutions.
(a) carbon spectra. (b) SiC spectra (O: Optic mode;
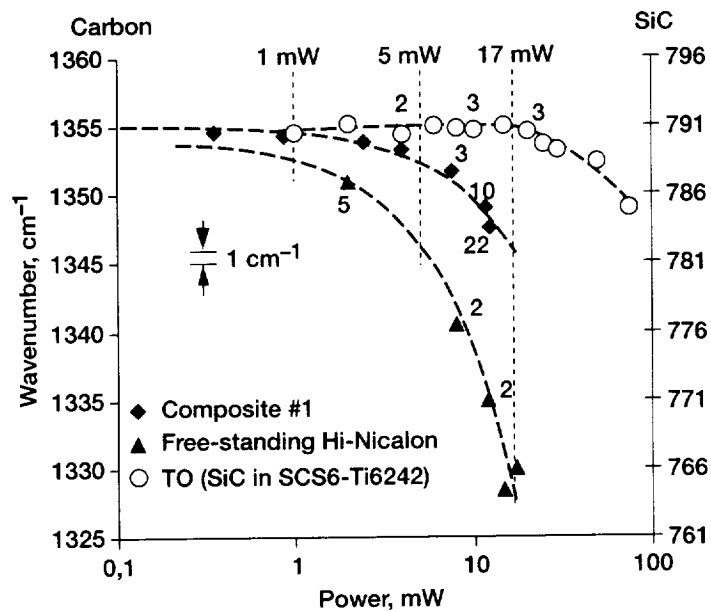T: Transverse mode; L: Longitudinal mode).

Figure 2.—Wavenumber versus laser power (λ = 514.5 nm) for the D band ("sp^3-sp^2/sp^3"-hybridized carbon atoms) of a Hi-Nicalon fiber (either free standing in air or embedded in composite #1; left-hand scale) and for SiC TO_1 mode in an SCS-6 fiber (right-hand scale). The labels indicate the number of measured values (when more than one) for the corresponding points. The displayed regression lines would be straight lines for a linear power scale.
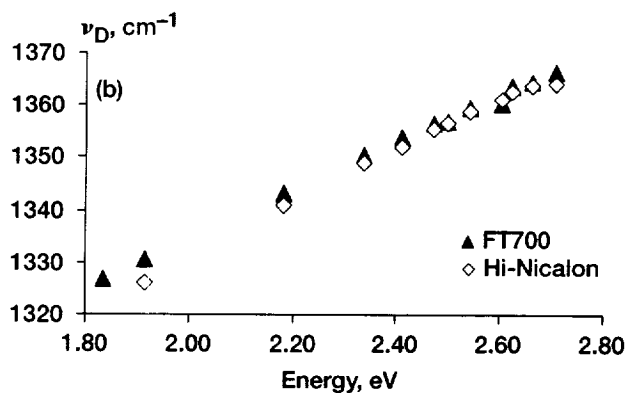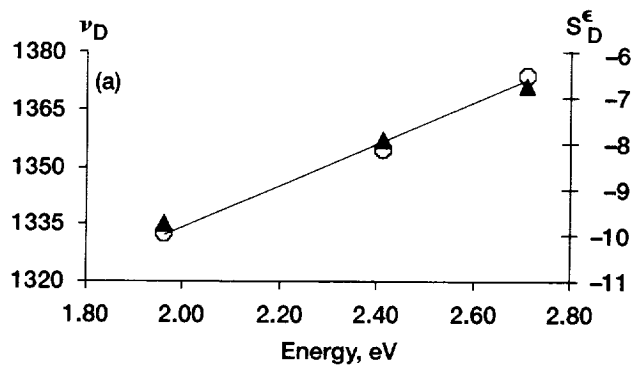
Figure 3.—(a) ν_D (left-hand scale, in cm^{-1}) and S$_D^\epsilon$ (right-hand scale, in cm^{-1} percent) as a function of the exciting laser line energy (in eV) for FT700 carbon fibers. (b) Comparison of ν_D dependency to the line energy in Hi-Nicalon and FT700 fibers.
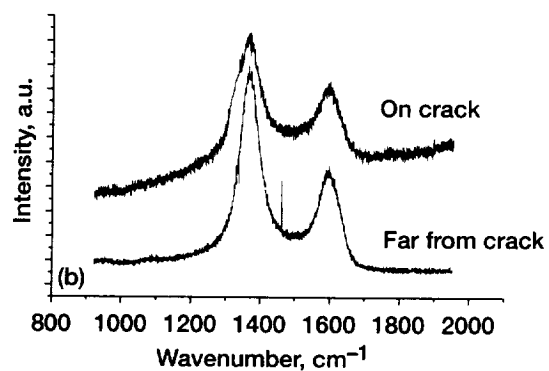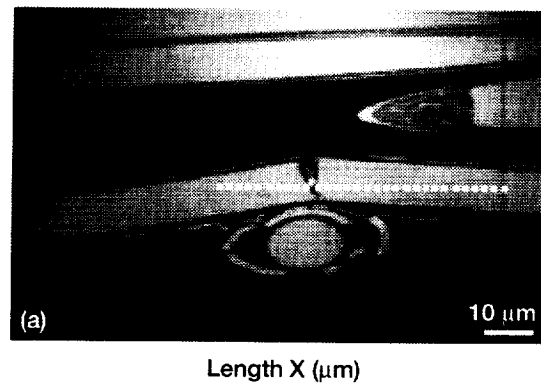

Figure 4.—(a) Photomicrograph of composite #2 polished parallel to the fiber direction. Spectra were recorded with the 458 nm line (5 mW, 60 seconds) at each point. (b) Examples of spectra recorded along the fiber and on the fiber crack.
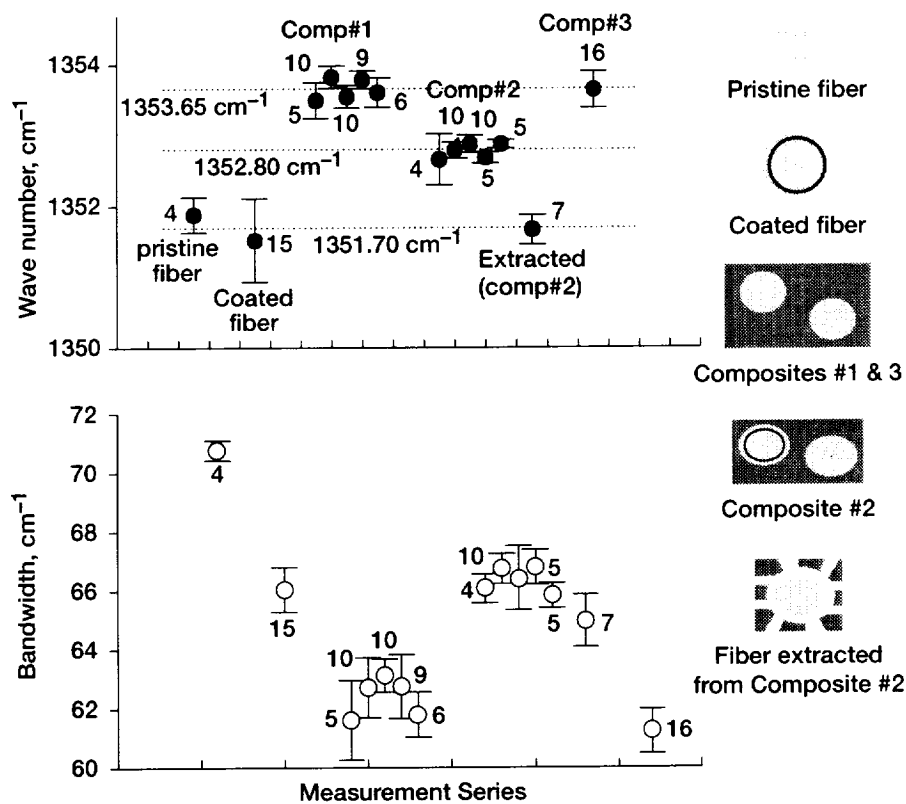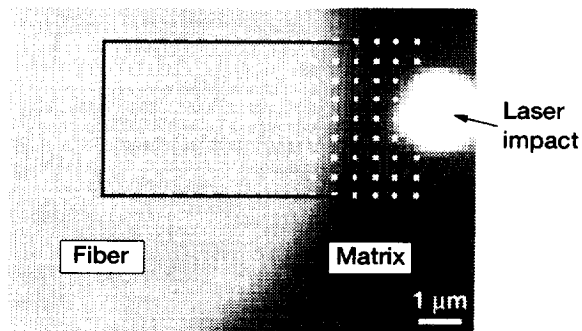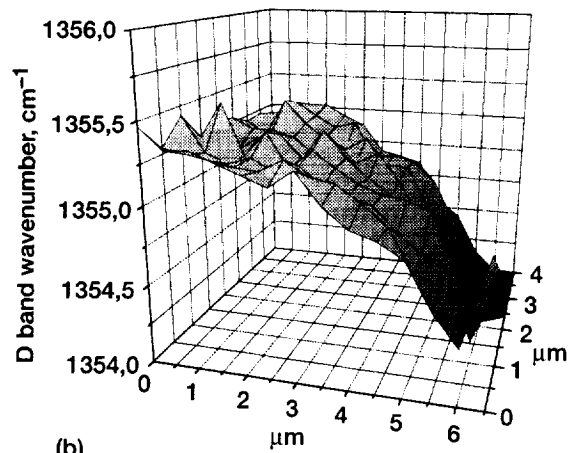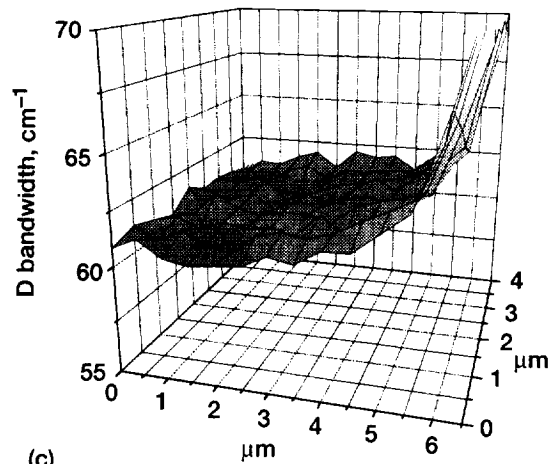
Figure 5.—Hi-Nicalon D band wavenumber (corrected by a neon reference line) and bandwidth determined by fitting the spectra recorded in 180 seconds (λ = 514.5 nm, P = 1 mW) on cross-sections of different samples (drawings on the right-hand side). Each point corresponds to a region selected in the corresponding sample. The number of recorded spectra is given.

Figure 6.—Example of cross section 2-D mapping
(0.5 μm steps in X and Y directions) performed on
a fiber/matrix interface in composite #1 (uncoated
fibers) using a 514.5 nm excitation (P = 1 mW,
t = 300 s). (a) Photomicrograph. (b) Mapping based
on the fitted wavenumbers for the spectra in the
black rectangle. (c) Bandwidth mapping.

REPORT DOCUMENTATION PAGE

Public reporting burden for this collection of information is estimated to average 1 hour per response, including the time for reviewing instructions, searching existing data sources, gathering and maintaining the data needed, and completing and reviewing the collection of information. Send comments regarding this burden estimate or any other aspect of this collection of information, including suggestions for reducing this burden, to Washington Headquarters Services, Directorate for Information Operations and Reports, 1215 Jefferson Davis Highway, Suite 1204, Arlington, VA 22202-4302, and to the Office of Management and Budget, Paperwork Reduction Project (0704-0188), Washington, DC 20503.

1. AGENCY USE ONLY (Leave blank)	2. REPORT DATE September 2000	3. REPORT TYPE AND DATES COVERED Technical Memorandum

4. TITLE AND SUBTITLE
Raman Study of Uncoated and p-BN/SiC-Coated Hi-Nicalon Fiber Reinforced Celsian Matrix Composites
Part 2: Residual Stress in the Fibers

5. FUNDING NUMBERS
WU–523–31–13–00

6. AUTHOR(S)
Gwénaël Gouadec, Philippe Colomban, and Narottam P. Bansal

7. PERFORMING ORGANIZATION NAME(S) AND ADDRESS(ES)
National Aeronautics and Space Administration
John H. Glenn Research Center at Lewis Field
Cleveland, Ohio 44135–3191

8. PERFORMING ORGANIZATION REPORT NUMBER
E–12441

9. SPONSORING/MONITORING AGENCY NAME(S) AND ADDRESS(ES)
National Aeronautics and Space Administration
Washington, DC 20546–0001

10. SPONSORING/MONITORING AGENCY REPORT NUMBER
NASA TM—2000-210456

11. SUPPLEMENTARY NOTES

Gwénaël Gouadec, Laboratoire Dynamique-Interactions-Réactivité (LADIR), UMR7075 - CNRS & Université Pierre et Marie Curie, Thiais, Val de Marne, 94320, France and Département Matériaux & Systèmes Composites (DMSC), Office National d'Etudes et de Recherches Aérospatiales (ONERA), Chatillon, Hauts de Seine, 92322, France; Philippe Colomban, Laboratoire Dynamique-Interactions-Réactivité (LADIR), UMR7075 - CNRS & Université Pierre et Marie Curie, Thiais, Val de Marne, 94320, France; and Narottam P. Bansal, NASA Glenn Research Center. Responsible person, Narottam P. Bansal, organization code 5130, (216) 433–3855.

12a. DISTRIBUTION/AVAILABILITY STATEMENT

Unclassified - Unlimited
Subject Category: 24   Distribution: Nonstandard

This publication is available from the NASA Center for AeroSpace Information, (301) 621–0390.

12b. DISTRIBUTION CODE

13. ABSTRACT (Maximum 200 words)

Band shifts on Raman spectra were used to assess, at a microscopic scale, the residual strain existing in Hi-Nicalon fibers reinforcing celsian matrix composites. Uncoated as well as p-BN/SiC- and p-B(Si)N/SiC-coated Hi-Nicalon fibers were used as the reinforcements. We unambiguously conclude that the fibers are in a state of compressive residual stress. Quantitative determination of the residual stress was made possible by taking into account the heating induced by laser probing and by using a reference line, of fixed wavenumber. We found fiber compressive residual stress values between 110 and 960 MPa, depending on the fiber/matrix coating in the composite. A stress relaxation-like phenomenon was observed at the surface of p-BN/SiC-coated Hi-Nicalon fibers whereas the uncoated or p-B(Si)N/SiC-coated Hi-Nicalon fibers did not show any stress relaxation in the Celsian matrix composites.

14. SUBJECT TERMS
Celsian; Silicon carbide fibers; Structural materials; Composites; Raman spectroscopy; Ceramics

15. NUMBER OF PAGES
22

16. PRICE CODE
A03

17. SECURITY CLASSIFICATION OF REPORT	18. SECURITY CLASSIFICATION OF THIS PAGE	19. SECURITY CLASSIFICATION OF ABSTRACT	20. LIMITATION OF ABSTRACT
Unclassified	Unclassified	Unclassified	